Carbohydrate Polymers 117 (2015) 1002–1013

Contents lists available at ScienceDirect

Carbohydrate Polymers

journal homepage: www.elsevier.com/locate/carbpol

# Structure of *Arabidopsis* leaf starch is markedly altered following nocturnal degradation

Fan Zhu [a,*], Eric Bertoft [b], You Wang [c], Michael Emes [c], Ian Tetlow [c], Koushik Seetharaman [b,1]

[a] School of Chemical Sciences, University of Auckland, Private Bag 92019, Auckland 1142, New Zealand
[b] Department of Food Science and Nutrition, University of Minnesota, 1334 Eckles Ave, St Paul, MN, USA
[c] Department of Molecular and Cellular Biology, University of Guelph, Guelph, Ontario, N1G 2W1, Canada

ARTICLE INFO

*Article history:*
Received 16 July 2014
Received in revised form
22 September 2014
Accepted 27 September 2014
Available online 17 October 2014

*Keywords:*
*Arabidopsis*
Transitory starch
Cluster
Structure
Thermal properties

ABSTRACT

Little is known about the thermal properties and internal molecular structure of transitory starch. In this study, granule morphology, thermal properties, and the cluster structure of *Arabidopsis* leaf starch at beginning and end of the light period were explored. The structural properties of building blocks and clusters were evaluated by using diverse chromatographic techniques. On the granular level, starch from end of day had larger granule size, thinner crystalline lamellae thickness, lower free surface energy of crystals, and lower tendency to retrograde than that from end of night. On the molecular level, the starch had lower amylose content, larger cluster size, and higher number of blocks per cluster at the end of day than at end of night. It is concluded that the core of the granules contains a more permanent molecular and less-ordered physical structure different from the transitory layers laid down around the core at daytime.



## 1. Introduction

In the context of plant physiology, there are two basic types of starch – transitory and storage. Transitory starch accumulates in the chloroplast tissue of leaves during the light period and is consumed in the dark period, whereas storage starch accumulates and is degraded over longer periods, providing energy and carbon for seed germination after dormancy (Smith, 2012). While much research has focussed on storage starch to determine its structure and functional properties, research on transitory starch has been more directed towards understanding its turnover through mutation and biochemical analysis (Stitt & Zeeman, 2012). In fact, there is a long history of research on starch in leaves. In 1837, von Mohl first observed starch granules in the chlorophyll-bodies of green plants (Brown & Morris, 1893). In 1862, Sachs showed the influence of light on the production of starch in the "chlorophyll-bodies" (chloroplasts), and that the appearance of starch in the chlorophyll-bodies is dependent on the action of light of sufficient intensity (Brown & Morris, 1893). Since these early pioneering discoveries, numerous studies have attempted to better illustrate the role of leaf starch in the plant metabolism (Santelia & Zeeman, 2011; Smith, 2012; Zeeman, Smith, & Smith, 2007). Nowadays, leaf starch from *Arabidopsis* has become the major model not only for further illustration of the nature of transitory starch, but also with a biotechnological target of using this weed as a model for improving agricultural and economic crops, in which storage starches predominate (Santelia & Zeeman, 2011; Zeeman et al., 2002).

In *Arabidopsis* leaves, the substrate for starch synthesis, ADP-glucose, is derived from the Calvin–Benson cycle. The ADP-glucose is used by five classes of starch synthases (SS) for elongation of α-glucan chains, which are then branched by two isoforms of starch branching enzyme (SBE), SBE 2.1 and 2.2 (Smith, 2012). Synthesis of the granules also requires two isoforms of debranching enzymes, namely the isoamylase (ISA) 1 and 2, which facilitate formation of the water-insoluble, semi-crystalline polymers (Smith, 2012). While the pathway of starch synthesis in leaves is broadly similar to that of the storage starches, the mechanism of starch degradation differs greatly in leaves and storage organs. Reversible glucan phosphorylation has been shown to be essential for starch degradation in chloroplasts (Fettke, Fernie, & Steup, 2012). Phosphorylation

* Corresponding author.
*E-mail address:* fzhu5@yahoo.com (F. Zhu).
[1] This publication is dedicated to the memory of Dr. Koushik Seetharaman (1966–2014).

http://dx.doi.org/10.1016/j.carbpol.2014.09.092
0144-8617/

at the C-6 and C-3 positions of the glucose units was suggested to play a role in starch metabolism by introducing strain in the crystalline lamellae and resulting in helix unfolding (Blennow & Engelsen, 2010). The disrupted glucan chains are further degraded by β-amylases and debranching enzymes, with the release of maltose and malto-oligosaccharides from the granule surface. Malto-oligosaccharides are further hydrolyzed by α-amylases and disproportionating enzyme in the stroma into glucose and maltose, which are exported into the cytosol for further utilization (Stitt & Zeeman, 2012).

Starch consists of semi-crystalline biopolymers simply made of glucose units that make up the two molecular components – amylose and amylopectin. The former is linear with α-(1→4) linkages and the latter is branched with ~5% α-(1→6) linkages (Pérez & Bertoft, 2010). The branches in amylopectin exist as clusters, which can be isolated by partial hydrolysis with α-amylase of *Bacillus amyloliquefaciens* (Bertoft, 2007a). Clusters were structurally defined as groups of chains, in which the internal chain length (ICL) between the branches is smaller than nine glucosyl residues (Bertoft, 2007b). The clusters consist of tightly branched building blocks, which are isolated as α-limit dextrins (α-LDs) (Bertoft, 2007b). The building blocks have between two and approximately 10 chains and ICL 1–3 (Bertoft, 2013). A series of systematic studies led to the proposition of a two-directional backbone model for the molecular structure of amylopectin, in which the clusters and building blocks represent the internal structure along the backbone (Bertoft, 2013). The model has been related to the physical structure and functionality of granular starch (Vamadevan, Bertoft, & Seetharaman, 2013a; Vamadevan, Bertoft, Soldatov, & Seetharaman, 2013b).

Many reports have been focused on the genetic and biochemical basis for the synthesis and degradation of *Arabidopsis* leaf starch. The structural changes of starch, especially the internal molecular structure, during the diurnal cycle are much less known. The internal molecular structure has been linked to the biosynthesis, structure, and functionality of starch granules based on the data from storage starch (Bertoft, 2013). It would thus be interesting to extend the analytical paradigm well established in the internal structure of storage starch to include transitory starch in order to better understand its nature. Reports on the structural and compositional changes of starch components from the end of day and end of night in leaves were described in some plants, such as potato (Santacruz, Koch, Andersson, & Åman, 2004), tobacco (Matheson & Wheatley, 1963), and cotton (Chang, 1979). In general, leaf starch has rather different structural features as compared with the storage starch, and the structure and composition is influenced by factors including the diurnal cycle, the sampling time point, as well as the maturity and developmental stage of the leaf (Chang, 1979; Matheson & Wheatley, 1963; Santacruz et al., 2004). While these reports do reveal certain structural features of leaf starch during the diurnal cycle, there is still a huge gap to be filled in order to better understand the fine structural nature of transitory starch, especially in *Arabidopsis*.

Compared with storage starch, much less is known about the functionality and internal structure of transitory starch, mostly due to the difficulty in acquiring sufficient amounts of starch for comprehensive analyses. The detailed analysis of cluster and building block structure of amylopectin normally requires a sufficient amount of sample (in grams) to separate amylopectin from amylose as the pre-requisite (Bertoft, 2007a, 2007b). Recent development in analytical methodology and conceptual breakthrough allows for using relatively small amount of samples (in milligrams) for reasonable characterization of the cluster and building block structure of starch without amylose and amylopectin separation (Zhu, Bertoft, & Seetharaman, 2013a; Zhu, Bertoft, & Seetharaman, 2014). This study reports on the thermal properties and molecular structure of *Arabidopsis* leaf starches collected from end of night and end of day.

## 2. Materials and methods

### 2.1. Leaf starches

Starches were all from the same inbred genetic background of *Arabidopsis* (Columbia). Starch was extracted based on the method described previously (Smith & Zeeman, 2006) from leaves collected at the beginning and end of light period (16 h light followed by 8 h night) after four weeks since planting seeds to ensure accumulation of starch and that the structural comparison between samples was significant.

### 2.2. Enzymes

α-Amylase of *Bacillus amyloliquefaciens* (EC 3.2.1.1), β-amylase of barley (EC 3.2.1.2, specific activity 705 U/mg), pullulanase of *Klebsiella pneumoniae* (EC 3.2.1.41, specific activity 699 U/mg), and isoamylase of *Pseudomonas amyloderamosa* (EC 3.2.1.68, specific activity 210 U/mg) were obtained from Megazyme (Wicklow, Ireland). The activity of the α-amylase (315 U/mL at pH 6.5, 25 °C) was determined based on a previous description (Bertoft, Manelius, & Qin, 1993). The given activities of other enzymes were reported by the suppliers.

### 2.3. Scanning electron microscopy (SEM)

Starch samples were mounted on circular aluminum stubs before sputter coated with palladium to ~20 nm thickness and were examined by a scanning electron microscope (Hitachi S-570, Hitachi High Technologies, Tokyo, Japan) at an accelerating voltage of 10 kV.

### 2.4. Differential scanning calorimetry (DSC)

Gelatinization properties of starches were measured by using TA Instruments, Q1000 differential scanning calorimeter equipped with a thermal analysis data station and data recording software (TA Instruments, Universal Analysis 2000, New Castle, Delaware). Starch dispersions in water (1:3) were equilibrated for 1 h at room temperature before DSC analysis. The sample was equilibrated at 10 °C for 5 min, then scanned from 10 to 110 °C at a heating rate of 2 °C/min.

Gelatinized starch was placed at 4 °C for 40 days to undergo retrogradation before rescan. The sample was equilibrated at 10 °C for 2 min, then scanned from 10 to 120 °C at a heating rate of 10 °C/min.

### 2.5. Isolation of clusters from leaf starches

Leaf starch (40 mg) was dissolved in 0.8 mL of 90% dimethyl sulfoxide (DMSO) by gentle heating and then stirring for two days at room temperature (~22 °C). Hot double-distilled water (2.8 mL) was added. After cooling, α-amylase (0.4 mL, 0.9 U/mL) in NaOAc buffer (0.01 M, pH 6.5) was added to start the reaction in a water bath (25 °C) with stirring. The reaction was continued for 85 min before termination by the addition of NaOH (80 μL, 5.0 M) and standing at room temperature for 3 h to destroy the α-amylase. Pure methanol (20 mL) was added to precipitate the α-dextrins of clusters. The sample was left at 4 °C for 3 h before the precipitate was recovered by centrifugation (4000 × g, 20 min) at room temperature. The precipitate was washed twice with pure methanol (5 mL) and stood in fume hood for 2 h to remove the methanol through evaporation.

The external chain remnants of α-dextrins of clusters were removed by β-amylase to obtain the β-LDs of clusters as previously described (Zhu et al., 2013a). The clusters in the form of

β-LDs were separated from maltose and the buffer salt on two PD-10 columns (GE Healthcare Life Sciences, NJ, USA) coupled in tandem (Kong, Corke, & Bertoft, 2009). The filtration through the PD-10 columns was done twice before the solution was condensed by rotary evaporation (50 °C) to a smaller volume to achieve a suitable carbohydrate concentration for further analyses and stored at −30 °C.

### 2.6. Isolation of building blocks from β-limit dextrins of clusters

β-LDs of clusters were diluted to 5.6 mg/mL by adding hot water before α-amylase (60 U/mL) in NaOAc buffer (0.01 M, pH 6.5) was added at 35 °C to start the reaction for 3 h to produce the building blocks. The concentrations for substrate and α-amylase during the incubation were 5 mg/mL and 6.0 U/mL, respectively. The reaction was stopped by boiling for 10 min. Then, β-amylase (1 μL) with NaOAc buffer (pH 6.0, 0.01 M, 0.3 vol.) was added to remove any remaining external chain segments. The β-amylolysis was conducted at 40 °C for 3 h before being stopped by boiling for 10 min. The building blocks in solution were stored at −30 °C before analysis.

### 2.7. Analysis of unit chains in clusters and building blocks by debranching

Solutions of clusters and building blocks (1 mg) were diluted in hot water (225 μL). After cooling, NaOAc buffer (25 μL, 0.01 M, pH 5.5), pullulanase (1 μL), and isoamylase (1 μL) were added. The reaction was at room temperature for 20 h with stirring to completely break the α-(1→6) linkages before analysis by HPAEC as described below. The reaction was terminated by boiling for 10 min.

### 2.8. Gel-permeation chromatography (GPC)

Starch (dissolved in 90% DMSO) was analyzed on a column (1.6 × 45 cm) of Sepharose 2B (Pharmacia, Uppsala, Sweden). The injection volume was ~500 μL with a carbohydrate content of ~2.0 mg. The eluent was NaOH (0.01 M) with a pumping speed of 0.5 mL/min. Every second fraction (0.5 mL) was analyzed for carbohydrate content by the phenol–sulfuric acid method (Dubois, Gilles, Hamilton, Rebers, & Smith, 1956). Every second fraction (0.5 mL) was also used to analyse $\lambda_{max}$ of the iodine-glucan complex following a previous description (Klucinec & Thompson, 1998). HCl (1 mL, 0.01 M) and 50 μL of iodine solution (0.5 g of $I_2$ and 0.05 g of KI/100 mL of water) were added to 0.5 mL sample. Absorbance was recorded between 450 to 800 nm by wavelength scanning.

Clusters were analyzed on a column (1.6 × 90 cm) of Sepharose CL 6B (GE Healthcare Life Sciences, NJ, USA). The eluent was NaOH (0.5 M) with a flow rate of 1.0 mL/min. The building blocks were analyzed on a column (1.6 × 90 cm) of Superdex 30 (GE Healthcare Life Sciences, NJ, USA) eluted with NaCl (0.05 M) at 1.0 mL/min. Fraction (1.0 mL) were analyzed for carbohydrate content by the phenol–sulfuric acid method (Dubois et al., 1956). The columns were calibrated with commercial linear dextrins of DP 1–7 (Supelco, Bellefonte, PA, USA) and with branched dextrins of known DP (DP > 11) prepared from starch α-hydrolysates of *B. amyloliquefaciens* as previously reported (Bertoft & Spoof, 1989).

### 2.9. High-performance anion-exchange chromatography (HPAEC)

Samples were analyzed by high-performance anion-exchange chromatography with pulsed amperometric detection (HPAEC-PAD) on a Dionex ICS 3000 instrument (Sunnyvale, CA, USA). The analytical column was CarboPac PA-100 (4 × 250 mm), combined with a CarboPac PA-100 guard column (4 × 50 mm). The flow rate was 1.0 mL/min and the injection volume was 25 μL with suitable carbohydrate concentration. The eluents were solutions A (0.15 M NaOH) and B (0.15 M NaOH, containing 0.50 M NaOAc). The unit chain length distribution of debranched clusters followed the gradient of eluent B: 0–9 min, 15–36%; 9–18 min, 36–45%; 18–110 min, 45–100% B. The analysis of building blocks followed the gradient of eluent B: 0–15 min, 15–34%; 15–26 min, 34–40%; 26–52 min, 40–49%; 52–54 min, 49–100%. The column was equilibrated with 15% eluent B for 60 min between runs. Samples were diluted in order to be in the linear range of response of the PAD detector with signal converted to carbohydrate content (Koch, Andersson, & Åman, 1998). The PAD signal is comparable for branched and linear dextrins with the same DP (Bertoft, 2007b). The position of the branched dextrins in the chromatograms was determined as previously described (Bertoft, 2007b).

### 2.10. Statistical analysis

Samples were collected in biological duplicate and data was collected in triplicate and analyzed using SPSS Version 19.0 software (IBM Corporation, Armonk, NY, USA). Differences between means of data were compared by Tukey's test at a significance level $p < 0.05$. In the tables, different small-cased letters within one column indicate significant differences ($p < 0.05$).

## 3. Results and discussion

### 3.1. Morphology of starch granules

Scanning electron microscopy (SEM) revealed that the *Arabidopsis* leaf starch granules from the end of day and end of night were flat and discoid in shape (Fig. 1). The size of granules from the end of day was approximately 2–3 μm in diameter and 1–1.5 μm at the end of night. The thickness of the granules was about 200–400 nm and the granules from the end of day appeared somewhat thicker than from the end of night. The general dimension and shape of the starch granules agreed with previous reports on the morphology of *Arabidopsis* leaf starches (Smith, 2012). However, differences in the extent of the impact of diurnal cycle on the size of starch granules between this study and some previous reports (Crumpton-Taylor, Grandison, Png, Bushby, & Smith, 2012; Howitt, Rahman, & Morell, 2006) were observed. This discrepancy may be attributed to factors such as genotype, plant maturity, environmental conditions, sample preparation methods for SEM analysis (e.g., employment of sputtering), and quantification method.

The small size and shape of leaf starch enables an efficient carbon-utilization for plant growth during the diurnal cycle, fulfilling the requirement of maintaining a large surface area in order to permit both rapid synthesis and rapid degradation (Grange, Hammond, & Andrews, 1989). The degradation of starch granules during the nocturnal period may be initiated from the surface in a "peeling-off" and time-dependent manner (Zeeman, Kossmann, & Smith, 2010). Longer period of darkness leads to smaller granule size (Smith, 2012). The same pattern was also observed in transitory starches from tobacco (Matheson & Wheatley, 1963).

### 3.2. Thermal characterization

Gelatinization properties of leaf starch are presented in Table 1. The gelatinization onset, midpoint, and conclusion temperatures ($T_o$, $T_m$, and $T_c$) and the melting enthalpy change ($\Delta H$) from end of night were all lower than that from end of day. Previous results on the gelatinization pattern of various storage starches suggested that, in general, starches with B-type crystallinity have higher $\Delta H$ than those with A-type crystallinity (Vamadevan et al., 2013a). Wattebled, Planchot, Dong, Szydlowski, Pontoire, Devin, Ball, and D'Hulst (2008) reported that *Arabidopsis* starch is B-type. However,

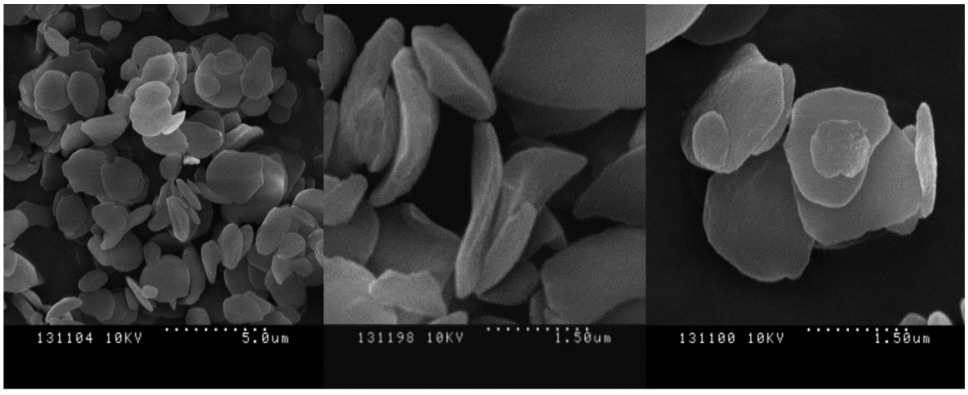


(a)

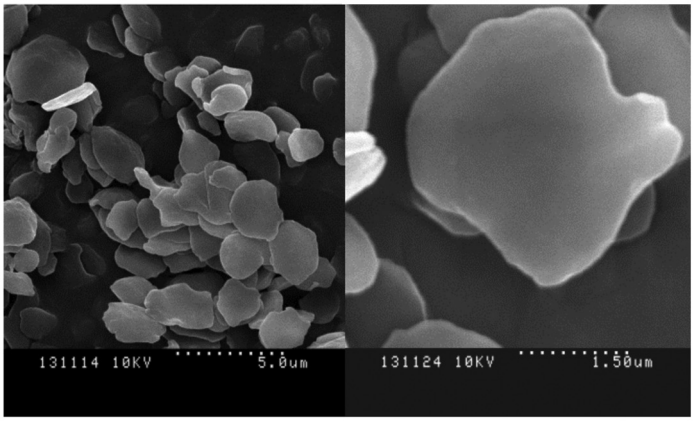


(b)

**Fig. 1.** Representative scanning electron micrographs of *Arabidopsis* leaf starches collected from end of night (a) and end of the day (b). Note that the SEM photos may be not able to reflect the decreased content of starch in the leaves at the end of night, and also note the different distance-bar shown in each photograph.

the $\Delta H$ of *Arabidopsis* leaf starch was in between the range previously observed for storage A- and B-type starches (Vamadevan et al., 2013a).

With a relatively low DSC scanning rate of temperature (e.g., 1 °C/min), gelatinization of starch–water dispersions can be considered as a quasi-equilibrium process where the "two-state" (native and molten) model is applicable for the description of the melting of crystalline lamellae (Kozlov, Blennow, Krivandin, & Yuryev, 2007). Even though the heating rate (2 °C/min) and starch concentration (25%) used here did not match the exact quasi-equilibrium process as suggested previously (Wang, Bogracheva, & Hedley, 1998), the data can still be used to calculate the relative, apparent crystalline structural parameters to reflect the trend (Shiotsubo & Takahashi, 1984). The model enables a calculation of the number of anhydroglucose residues in the crystalline lamellae ($\nu$), the thickness of the crystalline lamellae ($L_{crl}$), and the free surface energy of the crystals ($\gamma_i$) (Table 1). Leaf starch at end of night had more anhydroglucose residues in the crystalline lamellae (reflecting the cooperative melting unit) and thicker lamellae than at end of day. At the microscopic level, it was observed that the granules at the end of night were much smaller and thinner than at the end of day, apparently as a result of surface erosion (Zeeman, Kossmann, & Smith, 2010). This suggests that the internal component of the granules, which remained after the night, likely, has a different granular structure than the peripheral regions that were laid down during the day. It would also be interesting to measure the lamellae thickness by small-angle *X*-ray diffraction method in compared with the data from the DSC calculation. Analysis of starch by this method requires considerable amounts of starch (typically a few hundred mg) and was beyond the scope of the present study as *Arabidopsis* yields low quantities of starch.

Higher free surface energy ($\gamma_i$) reflects structural defects on the surface area of crystals, and the various possible structural defects formed on the crystals in starch granules as a result of α-glucan chain arrangements have been discussed previously by Kozlov et al. (2007). Crystals in the granules at end of night had higher $\gamma_i$ than at

**Table 1**
DSC characterization of *Arabidopsis* leaf starches.

| Sampling time | $T_o$ (°C) | $T_m$ (°C) | $T_c$ (°C) | $\Delta H$ (J/g) | Anhydroglucose residues ($\nu$) | $L_{crl}$ (nm) | $\gamma_i$ $10^{-7}$ (J/cm$^2$) |
|---|---|---|---|---|---|---|---|
| End of day | 53.0*a* | 57.0*a* | 62.8*a* | 14.5*a* | 14.5*b* | 5.1*b* | 6.1*b* |
| End of night | 51.9*b* | 55.9*b* | 61.3*b* | 11.2*b* | 17.6*a* | 6.2*a* | 7.9*a* |

$T_o$, $T_m$, and $T_c$ are onset, peak, and conclusion temperatures of gelatinization, respectively; $\Delta H$, melting enthalpy change; $L_{crl}$, thickness of crystalline lamellae; $\gamma_i$, free surface energy; the DSC analysis was conducted using a heating rate of 2 °C/min with a starch to water ratio at 1:3; different small-cased letters within a column indicate significant differences ($p < 0.05$).

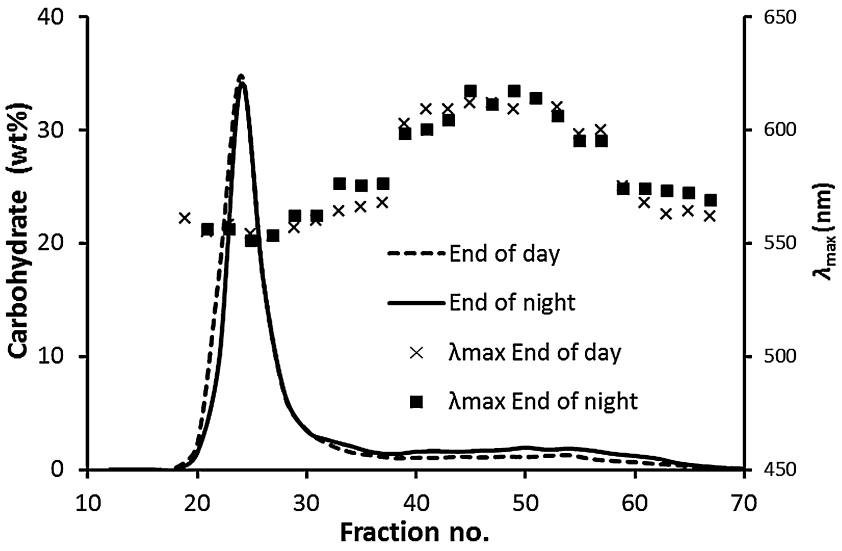


**Fig. 2.** Fractionation and iodine binding properties of whole starch on Sepharose CL 2B. Carbohydrate (wt%) indicates the weight percentage of carbohydrate content in each fraction.

end of day (Table 1). This suggested a comparatively rough surface on the crystals at end of night. Indeed, it was suggested that the crystalline lamellae are initially disrupted by the combined actions of glucan water dikinase (GWD) and phosphoglucan water dikinase (PWD) prior to degradation as starch is used for plant growth at night (Zeeman et al., 2010), and the surface properties of the starch at the end of the night may reflect a structure that has been subjected to the actions of these enzymes. On the other hand, it was recently claimed that GWD, in fact, is not involved in the starch degradation in *Arabidopsis* leaves at night (Skeffington, Graf, Duxbury, Gruissem, & Smith, 2014), and, therefore, the comparatively smoother surface of the crystals at end of day may simply reflect evenly built crystals during the day through a coordinated action of the diverse enzymes involved in starch biosynthesis.

The gelatinized starch was stored at 4 °C for 40 days before being rescanned by DSC for retrogradation analysis (Table 2). Retrogradation is affected by various factors, such as amylose content, amylopectin molecular structure, thermal history, water content, and other factors (Hoover, 2001). The melting temperatures ($T_o$, $T_m$, and $T_c$) of retrograded starch sampled from the end of night were higher than those from end of day, while the transition enthalpy change ($\Delta H$) exhibited the opposite trend. The degree of retrogradation (DOR), expressed as the ratio of $\Delta H$ of retrogradation to that of gelatinization, was higher for the sample from end of night (58%) than that from end of day (52%). This discrepancy clearly indicated the difference in the amylose/amylopectin composition and starch molecular structure as shown in the following sections.

**Table 2**
DSC characterization of retrogradation of *Arabidopsis* leaf starches.

| Sampling time | $T_o$ (°C) | $T_m$ (°C) | $T_c$ (°C) | $\Delta H$ (J/g) | DOR (%) |
|---|---|---|---|---|---|
| End of day | 43.2*b* | 56.7*b* | 71.6*b* | 7.6*a* | 52*b* |
| End of night | 44.5*a* | 57.6*a* | 72.2*a* | 6.5*b* | 58*a* |

$T_o$, $T_m$, and $T_c$ are onset, peak, and conclusion temperatures of retrogradation, respectively; $\Delta H$, melting enthalpy change; DOR, degree of retrogradation (%); different small-cased letters within a column indicate significant differences ($p < 0.05$).

### 3.3. Composition of amylose

Molecular size-distribution of the components and their iodine binding properties provide basic structural information of starch and the results are presented in Table 3 and Fig. 2. Iodine binding properties as reflected by $\lambda_{max}$ were comparable between starches from end of day and end of night, suggesting the structure of amylose (not the content of amylose) remained unaffected by diurnal cycle. Indeed, it was found in tobacco leaf starch that the starch-iodine binding properties were rather comparable between that at dawn and at dusk (Matheson, 1996). The $\lambda_{max}$ was ~ 560 nm for the amylopectin fractions and ~615 nm for amylose fractions. This agreed with previous reports on *Arabidopsis* leaf starch (Szydlowski et al., 2011). The apparent amylose contents measured by using GPC on Sepharose CL 2B were 18.5% for starch from end of day and 27.7% from end of night. Compared with another report on the apparent amylose content of *Arabidopsis* leaf starch measured by GPC on Sepharose CL 2B (Zeeman et al., 2002), the apparent amylose content from this study was much higher. This discrepancy may be attributed to the differences in the genotype and growth conditions.

The apparent amylose content was also measured by analyzing debranched starch by using GPC on Sepharose CL 6B and the results are present in Table 3 and Fig. 3. The apparent amylose contents measured by this method was 13.1% for starch from end of day and 17.4% from end of night, which were lower than when analyzed by using Sepharose CL 2B without debranching. This discrepancy agreed with previous reports on maize storage starches and may

**Table 3**
Characterization of amylose in *Arabidopsis* leaf starches.

| Sampling time | $AAM_{2B}$ (%) | $AAM_{6B}$ (%) | $LC_{AAM\text{-}6B}$ (%) | $SC_{AAM\text{-}6B}$ (%) | $LC_{AAM\text{-}6B}$:$SC_{AAM\text{-}6B}$ | $\lambda_{max}$ (nm) |
|---|---|---|---|---|---|---|
| End of day | 18.5*b* | 13.1*b* | 4.0*b* | 9.1*a* | 0.44*b* | 612*a* |
| End of night | 27.7*a* | 17.4*a* | 6.6*a* | 10.8*a* | 0.62*a* | 617*a* |

$AAM_{2B}$, apparent amylose content obtained by analysis of whole starch on Sepharose CL 2B; $AAM_{6B}$, apparent amylose content obtained by analysis of debranched starch on Sepharose CL 6B; $LC_{AAM}$, long chains of apparent amylose; $SC_{AAM}$, short chains of apparent amylose. $\lambda_{max}$, wave-length of maximum absorbance of the glucan-iodine complex obtained in fractions from gel-permeation chromatography on Sepharose CL 2B; different small-cased letters within a column indicate significant differences ($p < 0.05$).

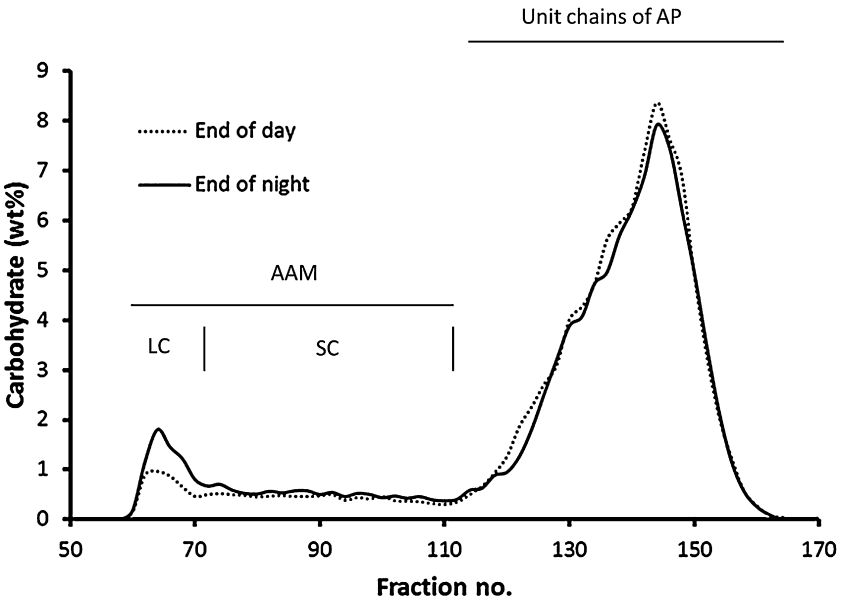


**Fig. 3.** Fractionation of debranched whole starches on Sepharose CL 6B. AAM, apparent amylose; LC, long chains of amylose; SC, short chains of amylose; AP, amylopectin. Carbohydrate (wt%) indicates the weight percentage of carbohydrate content in each fraction.

be attributed to the specific methods used (Zhu, Bertoft, Källman, Myers, & Seetharaman, 2013b). Apparent amylose can be categorized into long chains ($LC_{AAM\text{-}6B}$), eluting around the void volume on Sepharose CL 6B (fractions 56–70), and short chains ($SC_{AAM\text{-}6B}$), eluting between $LC_{AAM\text{-}6B}$ and amylopectin unit chains (fractions 72–110, Fig. 3). $LC_{AAM\text{-}6B}$ of leaf starch from end of day was lower (4.0%) than that from end of night (6.6%), whereas $SC_{AAM\text{-}6B}$ was similar. This resulted in a higher ratio of $LC_{AAM\text{-}6B}$:$SC_{AAM\text{-}6B}$ for leaf starch from end of night (0.62 *vs* 0.44).

The higher amount of amylose at dawn in *Arabidopsis* leaf starch agreed with previous data from tobacco (Matheson, 1996; Matheson & Wheatley, 1963) and cotton leaf (Chang, 1979) starches. This proportional difference in amylose and amylopectin content at end of night and end of day suggests that during the day more branched polymers resembling amylopectin are synthesized preferentially and these molecules are degraded during the night time resulting in a higher apparent amylose content.

β-LDs of whole starch were also debranched and analyzed by GPC on Sepharose CL 6B (Fig. 4). The lower proportion of chains between fractions 110 and 145 at the end of night and consequent higher maltose content suggested a higher proportion of external chains. Furthermore, trace amounts of longer chains (fractions 56–110) were observed, suggesting the presence of branched amylose and/or super-long unit chains of amylopectin.

### 3.4. Molecular structure of the clusters

Whole starch was subjected to partial α-amylolysis to isolate clusters in the form of α-dextrins, and the external parts of these α-dextrins were further removed by β-amylolysis to obtain the β-LDs of clusters, using previously described methods (Zhu et al., 2013a). The molecular size distribution of the β-LDs of clusters was analyzed by GPC on Sepharose CL 6B (Fig. 5), and the unit chain length distribution was analyzed by HPAEC after debranching (Fig. 6). From these two sets of data, various structural parameters were calculated (Table 4). Starch from end of day had larger clusters (DP = 63.7) with higher average chain length (CL = 5.9), internal chain length (ICL = 3.3), and total internal chain length (TICL = 9.1) than that from end of night (DP = 54.3, CL = 5.1, ICL = 2.5, and TICL = 8.0). The average number of chains in the clusters (NC) was, however, similar at the end of the night as at the end of the day. Compared with clusters from previously analyzed storage starches (Bertoft, Koch, & Åman, 2012), the cluster sizes of leaf starch, which has a B-type diffraction pattern (Wattebled et al., 2008), were similar to that of storage starches with the same diffraction pattern, but smaller than clusters from most A-type storage starches.

The unit chains of the clusters can be divided into different categories (Fig. 6) (Bertoft et al., 2012), and the molar distribution of these categories is summarized in Table 5. Leaf clusters from end of night had higher amounts of a- and b0-chains and less of b1- and b2-chains than at end of day. *Arabidopsis* leaf clusters had higher amounts of short b-chains (b0 and b1) compared with clusters from storage starches (Bertoft et al., 2012).

### 3.5. Structure of building blocks in the clusters

The β-LDs of clusters were extensively hydrolysed with α-amylase from *B. amyloliquefaciens* to produce α-LDs, also termed

**Table 4**
Characterization of β-LDs of clusters from *Arabidopsis* leaf starches.

| Sampling time | DP | NC | CL | ICL | TICL |
|---|---|---|---|---|---|
| End of day | 63.7*a* | 10.8*a* | 5.9*a* | 3.3*a* | 9.1*a* |
| End of night | 54.3*b* | 10.5*a* | 5.1*b* | 2.5*b* | 8.0*b* |

DP, average degree of polymerization (DP) estimated by GPC; NC, number of chains estimated as DP/CL; CL, average chain length estimated by HPAEC; ICL, internal chain length = (CL − ECL) × NC/(NC − 1) − 1, in which ECL is 2 for β-limit dextrin; TICL, total internal chain length = CL of b-chains in β-LD − 1.5; different small-cased letters within a column indicate significant differences ($p < 0.05$).

**Table 5**
Molar distribution of diverse chain categories in β-LDs of clusters from *Arabidopsis* leaf starches.

| Sampling time | Chain categories (mole%) | | | | |
|---|---|---|---|---|---|
| | a | b0 | b1 | b2 | b3 |
| End of day | 55.0*b* | 13.1*b* | 28.0*a* | 2.9*a* | 1.0*a* |
| End of night | 58.8*a* | 19.8*a* | 18.1*b* | 2.0*b* | 1.3*a* |

DP range of a = 2–3, b0 = 4–6, b1 = 7–18, b2 = 19–27, b3 ≥ 28 for diverse unit chain categories; different small-cased letters within a column indicate significant differences ($p < 0.05$).

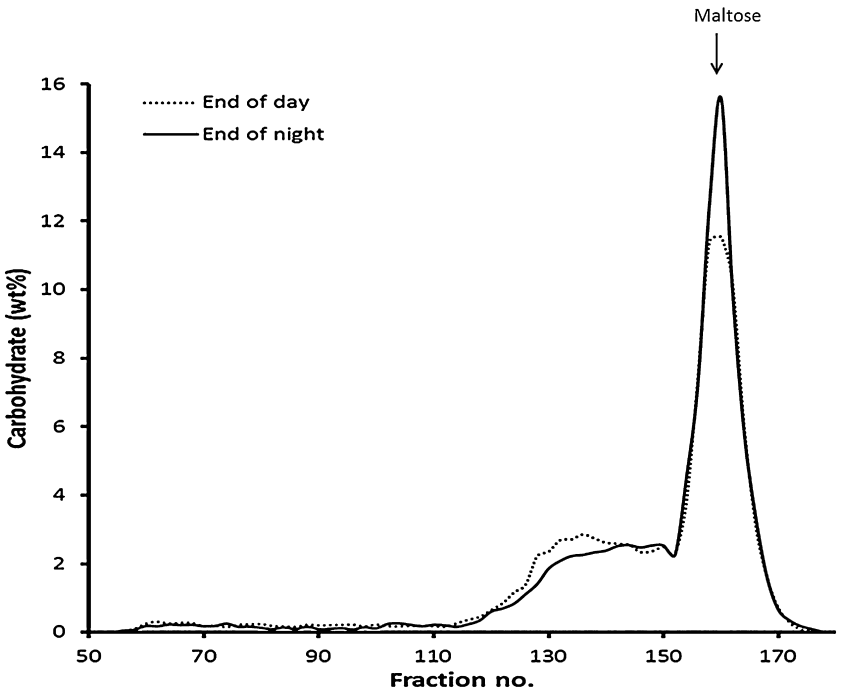


**Fig. 4.** Fractionation of debranched β-limit dextrins of whole starches on Sepharose CL 6B. Carbohydrate (wt%) indicates the weight percentage of carbohydrate content in each fraction.

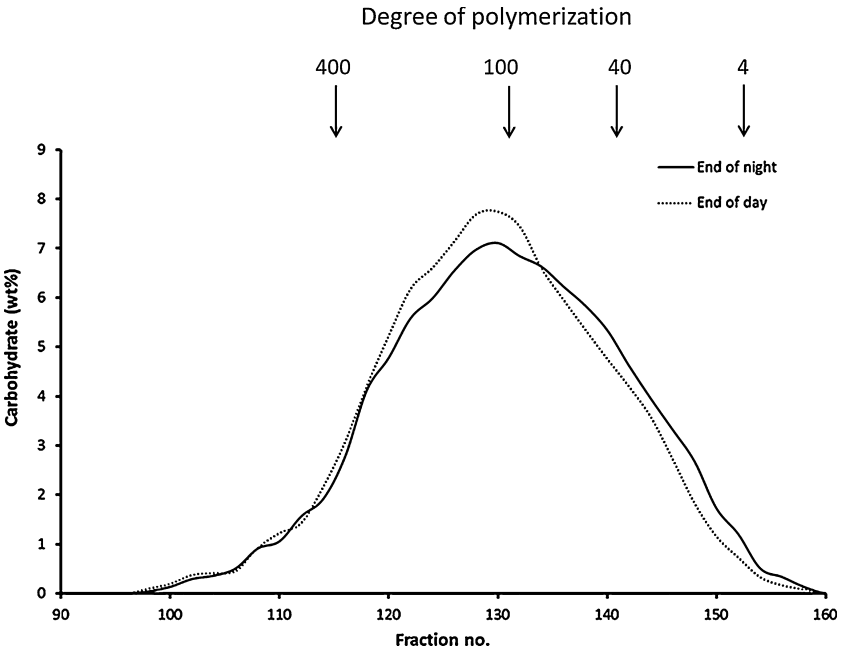


**Fig. 5.** Molecular size distribution obtained by GPC on Sepharose CL 6B of β-limit dextrins of clusters. The molecular markers (DP) for the molecular size of the dextrins were noted on the top of the figure. Carbohydrate (wt%) indicates the weight percentage of carbohydrate content in each fraction.

**Table 6**
Characterization of building blocks in β-LDs of clusters from *Arabidopsis* leaf starches.

| Sampling time | Linear | Branched | | | | | | | |
|---|---|---|---|---|---|---|---|---|---|
| | Mole (%) | DP | Wt (%) | Mole (%) | DP | NC | CL | ICL | TICL |
| End of day | 59.9*a* | 2.1*a* | 80.5*b* | 40.0*b* | 9.7*a* | 2.5*a* | 3.9*a* | 2.2*a* | 4.7*a* |
| End of night | 58.6*b* | 2.0*a* | 81.9*a* | 41.4*a* | 9.8*a* | 2.4*a* | 4.0*a* | 2.3*a* | 4.8*a* |

Linear dextrins have DP 1, 2, and 3, and branched building blocks have DP ≥ 5. DP, average DP estimated by GPC; CL, average chain length estimated by HPAEC; ICL, internal chain length = (CL − ECL) × NC/(NC − 1) − 1, in which external chain length (ECL) is estimated as 2; TICL, total internal chain length; NC, number of chains = DP/CL; different small-cased letters within a column indicate significant differences ($p < 0.05$).

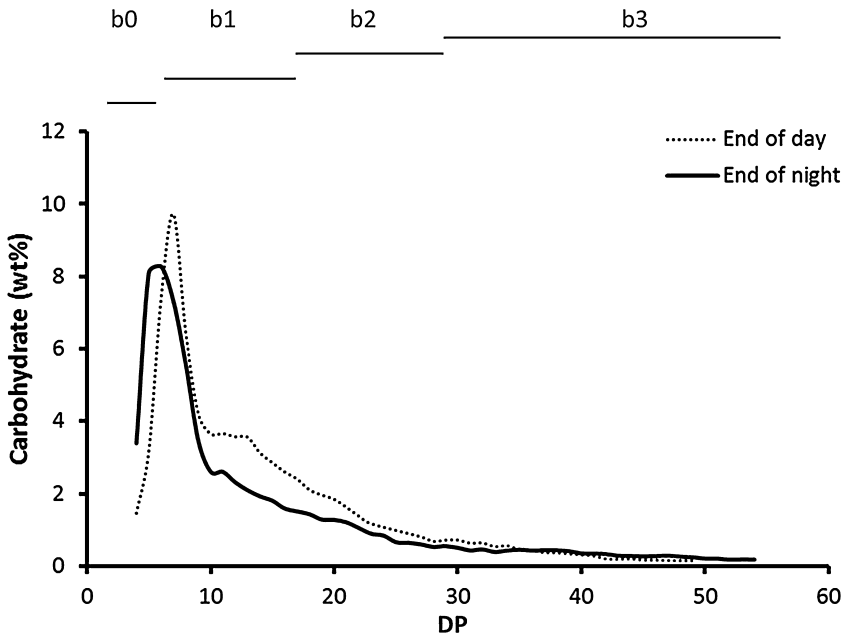


**Fig. 6.** HPAEC fractionation of internal unit chain length distribution of β-limit dextrins of clusters. DP range of b0 = 4–6, b1 = 7–18, b2 = 19–27, b3 ≥ 28. Carbohydrate (wt%) indicates the weight percentage of carbohydrate content in each fraction.

"building blocks" (Bertoft, 2007b). The composition of building blocks in the clusters were analyzed by GPC on Superdex 30 (Fig. 7) and also by HPAEC before (Fig. 8) and after debranching (Fig. 9). Molecular size distribution analysis revealed two distinct populations of dextrins. The smaller dextrins (population L) are linear dextrins released from the segments linking the branched blocks (population B) together (Fig. 7). Even though there is no sharp baseline separation between these two populations, the data from GPC are useful for the calculation of the average distance between the branched building blocks as described previously (Bertoft, Laohaphatanalert, Piyachomkwan, & Sriroth, 2010). The molar amount of the linear fraction in the clusters from end of day was somewhat higher than that from end of night (Table 6 and Fig. 7). The branched blocks had similar molecular structure at end of day and at the end of night (Table 6).

The building block structure of the clusters is shown in Table 7. The inter-block chain length (IB-CL) of clusters from end of day (7.1) was slightly higher than at end of night (6.8). Clusters from

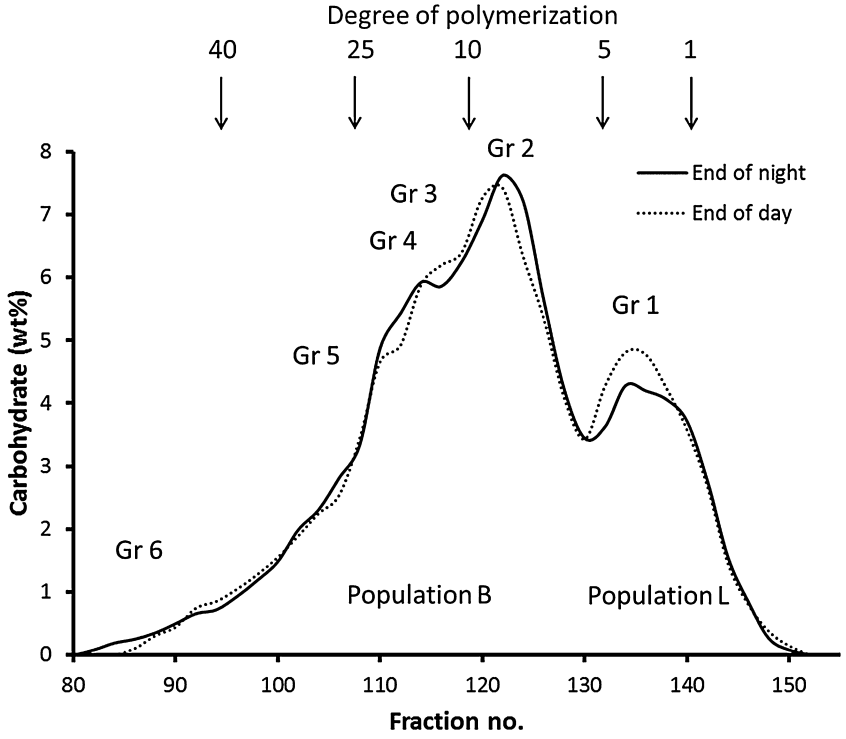


**Fig. 7.** Fractionation of building blocks in clusters by GPC on Superdex 30. The dextrins are categorized as branched (Population B) and linear (Population L) and divided into six groups (Gr 1, which consists of glucose, maltose, and maltotriose, and the branched Gr 2 with 2 chains and DP 5–9, Gr 3 with 3 chains, DP 10–14, Gr 4 with 4 chains, DP 15–19, and groups 5, DP 20~35, and 6, DP > 35, with ≥5 chains). Carbohydrate (wt%) indicates the weight percentage of carbohydrate content in each fraction.

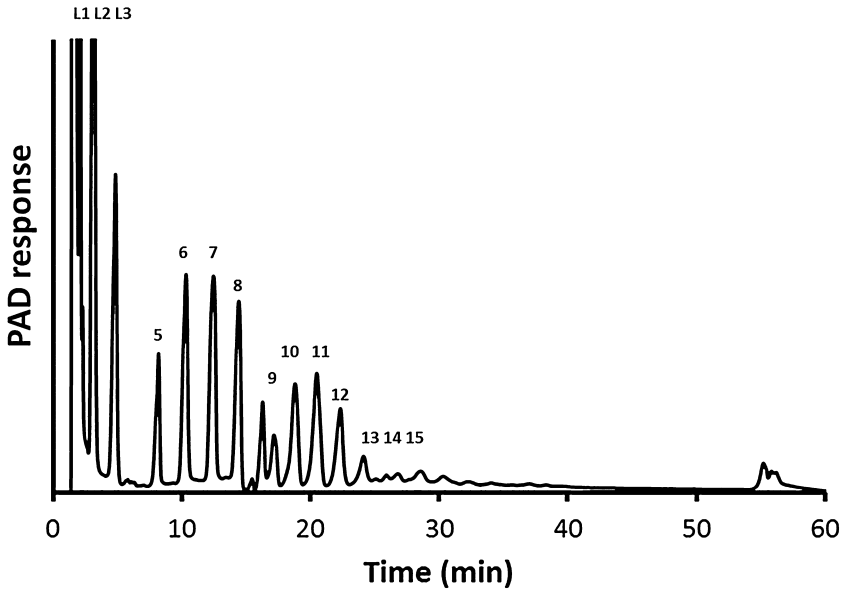


**Fig. 8.** HPAEC fractionation of building blocks of starch of the end of day. Indication of the nature and DP of building blocks are illustrated where L1, L2, and L3 ("L" for linear dextrin) denote glucose, maltose, and maltotriose, respectively, and the rest are branched dextrins with respective DP up to DP 15. PAD response indicates the signal from the pulsed amperometric detection. The nature of the last peak eluted around 56 min was discussed previously (Bertoft, 2007b).

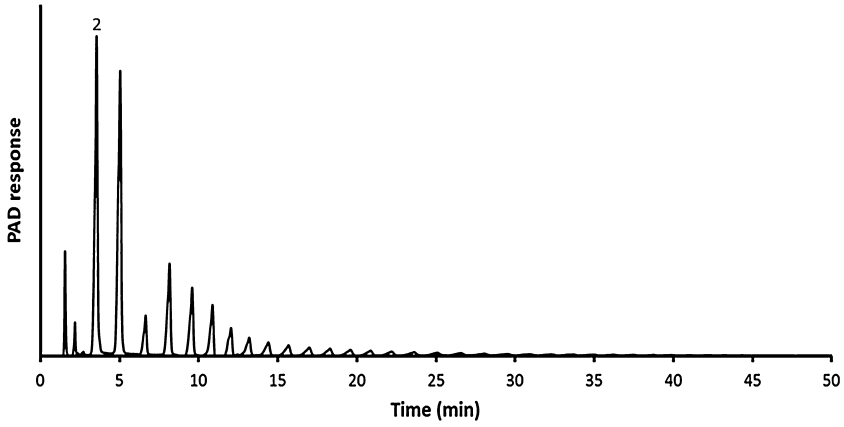


**Fig. 9.** HPAEC fractionation of debranched β-LD of clusters from end of night. Unit chain length of DP 2 (maltose) is indicated. PAD response indicates the signal from the pulsed amperometric detection.

end of day contained more building blocks per cluster (NBbl = 4.7) than at end of night (4.0) but had similar density of building blocks (DBbl = 7.4). Branched blocks can be categorized into five groups (2–6) with increasing number of chains per block (Bertoft, 2007b). Molar distribution of each block category was obtained from GPC on Superdex 30 (Fig. 7). Clusters isolated from the end of day and end of night had similar proportions of the diverse groups of blocks (Table 7).

Previous studies revealed a correlation between the average distance between the building blocks in clusters and the type of crystallinity of storage starches (Bertoft et al., 2012). Thus, IB-CL in B-type starches is generally higher than in A-type starches. Furthermore, in this study, IB-CL fell into the range of B-type starches (Table 7), which suggests that the general principle also is valid for transitory starch. Storage starches from diverse botanical origins (e.g., cereals, beans, and tubers) (Bertoft et al., 2012) and *Arabidopsis* leaf starch had comparable structure of the building blocks. However, the latter had higher amount of the smallest building blocks with only two chains (group 2) and less of the larger, multiple-branched blocks in groups 5 and 6. Compared with the larger blocks,

**Table 7**
Composition of building blocks in β-LDs of clusters from *Arabidopsis* leaf starches.

| Sampling time | IB-CL | DBbl | NBbl | Distribution of block categories (mole%) | | | |
|---|---|---|---|---|---|---|---|
| | | | | Group 2 | Group 3 | Group 4 | Groups 5–6 |
| End of day | 7.1*a* | 7.4*a* | 4.7*a* | 63.8*a* | 23.8*a* | 7.5*a* | 4.9*a* |
| End of night | 6.8*b* | 7.4*a* | 4.0*b* | 64.1*a* | 23.4*a* | 7.6*a* | 4.8*a* |

IB-CL, inter-block chain length per cluster = $mole\%_{linear} \times DP_{linear}/mole\%_{branched} + 4$; DBbl, density of building blocks per cluster = $NBbl/DP_{cltr} \times 100$, in which $DP_{cltr}$ is the average DP of φ,β-LDs of clusters; NBbl, number of building blocks per cluster = $wt\%_{Bbl}/100 \times DP_{cluter}/DP_{Bbl}$, in which $wt\%_{Bbl}$ is the weight percent of branched building blocks; categorization of groups 2–6 of building blocks based on their number of chains per block (i.e., group 2 has two chains and DP 5–9, group 3 has three chains, DP 10–14, group 4 has four chains, DP 15–19, and groups 5 and 6 have ≥ five chains and DP ≥20); different small-cased letters within a column indicate significant differences ($p < 0.05$).

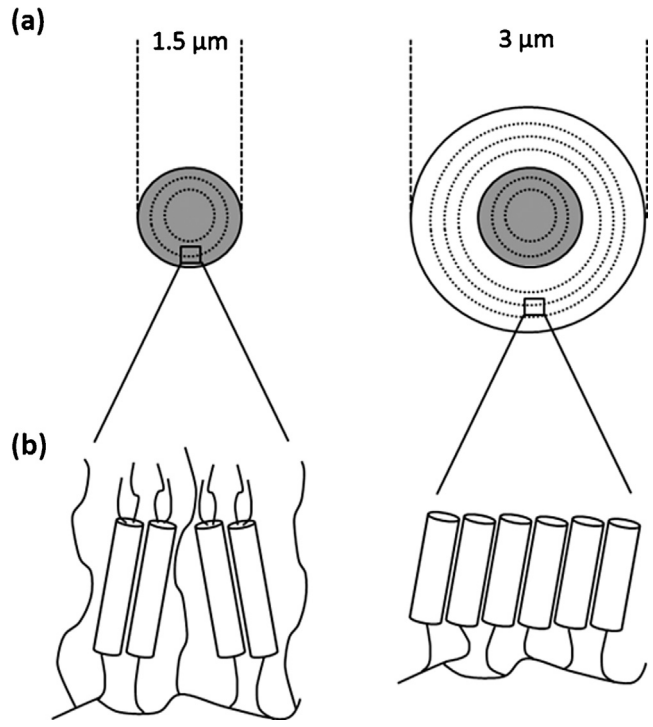


**Fig. 10.** Schematic representations of the starch granule at end of night (left) and end of day (right). (a) The granule consists of a structured core at end of night and has additional ordered layers at end of day. Note that the sphere shape of granules is only of a schematic illustration rather than the actual situation where the shape is flattened and disc-like. (b) The crystalline lamellae are thicker and smaller with rough surface and low enthalpy change at the core and are thinner but larger and with more ordered structure at end of day. Cylinders represent double helices in crystalline lattices.

the singly branched blocks of group 2 might be more readily subjected to degradation and amenable for utilization in nocturnal plant metabolism, fulfilling the transitory nature of leaf starch.

### 3.6. *Does the diurnal cycle reveal information about starch structure and granular architecture?*

The transitory starch granules in *Arabidopsis* are subjected to constant metabolic turnover. As expected, the starch content in the leaves at the end of night drastically decreased as compared to that at the end of day in this study. This process is under circadian control to ensure that starch availability is maintained until the next dawn and has been well documented (Crumpton-Taylor, Grandison, Png, Bushby, & Smith, 2012; Graf, Schlereth, Stitt, & Smith, 2010; Howitt, Rahman, Morell, 2006; Smith, 2012), and thus was not a focus of the current research.

The starch granules in the chloroplasts of *Arabidopsis* appear to be uniformly degraded and become smaller while the granule number remains relatively constant during the night (Crumpton-Taylor et al., 2012). Granular structure remains, or the central cores of granules, following overnight degradation of the outer layers had characteristics of normal granules, i.e., they were partly crystalline as shown by gelatinization, which resulted in an endothermic enthalpy change due to the melting of external chains in the form of crystalline lamellae. These lamellae had apparent thickness of approximately 6.2 nm, which corresponds to 17.2 anhydroglucose units (Table 1). During daytime new layers of starch were synthesized upon the core granules remaining after the night. The remaining core is schematically illustrated in Fig. 10a. The diameter of the granules at the end of day suggested that the proportion of these new layers represented roughly 4–7 times the volume of the core. This suggested that the measured parameters of starch at end of day mostly represent these new layers, albeit being a mixture with the starch in the core. Therefore, it was of interest to notice that the crystalline lamellae were thinner at the end of day (5.1 nm) and the surface free energy of the crystals was lower compared to end of night, but the melting enthalpy change was higher at end of day (Table 1). This suggested that larger crystals with shorter and more perfectly ordered chains were formed during the day, and were then degraded during the night. As a result, at the end of night a core remained with thicker crystalline lamellae, more defects, and higher surface roughness, possibly with smaller lateral size as well (Fig. 10b). Indeed, the hilum region of storage starch granules is much less ordered near the center as revealed by atomic force microscopy (AFM) study (Baker, Miles, & Helbert, 2001).

During starch degradation at night, the apparent amylose content of the residual structures (AAM) increased. The increased value based on GPC of whole starch was larger than that based on GPC of debranched starch (Table 3 and Fig. 2 and 3). The amylose, especially a small part of the polymers with intermediate hydrodynamic volume (fractions ~33–37, Fig. 2), possessed higher $\lambda_{max}$ values at end of night than at end of day. In addition, more maltose was produced by β-amylolysis at end of night, which suggested proportionally more of linear polymers and/or longer external chains in branched polymers. Such longer external chain segments could give rise to the physical properties of the crystalline lamellae at end of night (Fig. 10b).

It appears, therefore, that the structure of the polymer components was not identical in the core of the granules and in the outer layers produced during the daytime. We hypothesize that the core of the granules contains more of intermediate type of polymer structures and represents very early stages in granule development. The structure is possibly related to transitory starch granules observed in the wheat pericarp tissue. The starch from wheat pericarp tissue was shown to consist of polymers with intermediate structures characterized as highly branched chains of lengths found in amylose, but with overall structures intermediate to that of typical amylose and amylopectin (Kalinga et al., 2013). Wheat endosperm at early stages of development contains tiny, immature starch granules with similar structural characteristics (Kalinga et al., 2014). These granules have well-developed crystalline structures with thick lamellae and rough surface, and the blocklets are large with fuzzy contours that might relate to intermediate polymers (Waduge, Xu, Bertoft, & Seetharaman, 2013; Waduge, Kalinga, Bertoft, & Seetharaman, 2014).

Phosphorylation is essential for hydrolysis of starch in *Arabidopsis* and regulates starch metabolism (Blennow & Engelsen, 2010). Phosphorylated clusters in potato amylopectin are larger than their non-phosphorylated counterparts and have more long chains and longer CL and ICL (Wikman, Larsen, Mohammed, Blennow, & Bertoft, 2011). In *Arabidopsis* starch the clusters were larger and possessed longer CL and ICL at end of day than at end of night. This suggests that the clusters synthesized during the day might be more phosphorylated and readily degraded during night as needed. Conversely, the core of the granules might contain less phosphorylated clusters, which would retard or prevent hydrolysis of the core as this is needed as a platform for the synthesis of new starch polymers during daytime. Indeed, it must be mentioned that starch phosphorylation is not only involved in starch degradation but also in starch biosynthesis (Skeffington et al., 2014). To obtain a more wholesome picture, other factors (e.g., the location of the phosphate group in starch chains) affecting the cluster structure should be better explored.

It should be noted that starch granules mostly differ in their biochemical properties depending on particle size. Though a standard starch granule does not likely exist in the plant, the granules share

a lot of common structural features (e.g., susceptibility to degradation during night) (Crumpton-Taylor et al., 2012). The model present here (Fig. 10) is thus an assumption with the purpose of biologically reflecting the actual trend of the impact of diurnal cycle on starch structure. Another point is that starch biosynthesis in *Arabidopsis* proceeds relatively slowly under a 16 h light and 8 h dark period as compared with other daily patterns with different day lengths (Graf et al., 2010). It would thus be interesting to study if this type of structural evolution of leaf starch still holds during other rates of glucan deposition.

## 4. Conclusions

The diurnal cycle influences the structural and thermodynamic properties of *Arabidopsis* leaf starch. During the night, granule size decreases and the remnants of the granules at the end of night contain more amylose or longer chains that comprise the core of the granules. Clusters isolated from end of the night have a more dense structure with more short b-chains (DP < 7), less longer b-chains, less number of blocks per cluster, shorter inter-block chain length (IB-CL), and smaller size compared with that from end of day. Despite these differences, some features, including the molecular composition of building block in clusters and the chemical structure of building blocks, were not affected by nocturnal degradation. It appears that the core of the granules has a specific and less-ordered physical structure, upon which the transitory portion of starch with more-ordered structure is laid down during daytime and recycled into the metabolic pathways at night.

## Acknowledgments

Kind advice on the DSC calculation from Dr. Varatharajan Vamadevan is gratefully acknowledged. The research was supported by the Natural Sciences and Engineering Research Council of Canada(NSERC).

## References

Baker, A. A., Miles, M. J., & Helbert, W. (2001). Internal structure of the starch granule revealed by AFM. *Carbohydrate Research*, *330*, 249–256.
Bertoft, E. (2007 a). Composition of clusters and their arrangement in potato amylopectin. *Carbohydrate Polymers*, *68*, 433–446.
Bertoft, E. (2007 b). Composition of building blocks in clusters from potato amylopectin. *Carbohydrate Polymers*, *70*, 123–136.
Bertoft, E. (2013). On the building block and backbone concepts of amylopectin structure. *Cereal Chemistry*, *90*, 294–311.
Bertoft, E., & Spoof, L. (1989). Fractional precipitation of amylopectin alpha-dextrins using methanol. *Carbohydrate Research*, *189*, 169–180.
Bertoft, E., Koch, K., & Åman, P. (2012). Building block organisation of clusters in amylopectin from different structural types. *International Journal of Biological Macromolecules*, *50*, 1212–1223.
Bertoft, E., Laohaphatanalert, K., Piyachomkwan, K., & Sriroth, K. (2010). The fine structure of cassava starch amylopectin. Part 2: Building block structure of clusters. *International Journal of Biological Macromolecules*, *47*, 325–335.
Bertoft, E., Manelius, R., & Qin, Z. (1993). Studies on the structure of pea starches. Part 1: Initial stages in α-amylolysis of granular smooth pea starch. *Starch*, *45*, 215–220.
Blennow, A., & Engelsen, S. B. (2010). Helix-breaking news: Fighting crystalline starch energy deposits in the cell. *Trends in Plant Science*, *15*, 236–240.
Brown, H. T., & Morris, G. H. (1893). A contribution to the chemistry and physiology of foliage leaves. *Journal of the Chemical Society Transactions*, *63*, 604–677.
Chang, C. W. (1979). Starch and its component ratio in developing cotton leaves. *Plant Physiology*, *63*, 973–977.
Crumpton-Taylor, M., Grandison, S., Png, K. M. Y., Bushby, A. J., & Smith, A. M. (2012). Control of starch granule numbers in Arabidopsis chloroplasts. *Plant Physiology*, *158*, 905–916.
Dubois, M., Gilles, K. A., Hamilton, J. K., Rebers, P. A., & Smith, F. (1956). Colorimetric method for determination of sugars and related substances. *Analytical Chemistry*, *28*, 350–356.
Fettke, J., Fernie, A. R., & Steup, M. (2012). Transitory starch and its degradation in higher plant cells. In I. J. Tetlow (Ed.), *Starch, origins, structure and metabolism, SEB Essential Review Series* (5) (pp. 311–374). London: Society for Experimental Biology.
Graf, A., Schlereth, A., Stitt, M., & Smith, A. M. (2010). Circadian control of carbohydrate availability for growth in *Arabidopsis* plants at night. *Proceedings of the National Academy of Sciences of the United States of America*, *107*, 9458–9463.
Grange, R., Hammond, B., & Andrews, J. (1989). Characteristics of starch grains isolated from mature pepper leaves grown under different irradiances and day lengths. *Journal of Experimental Botany*, *40*, 1052–1945.
Hoover, R. (2001). Composition, molecular structure and physicochemical properties of tuber and root starches: A review. *Carbohydrate Polymers*, *45*, 253–267.
Howitt, C. A., Rahman, S., & Morell, M. K. (2006). Expression of bacterial starch-binding domains in *Arabidopsis* increases starch granule size. *Functional Plant Biology*, *33*, 257–266.
Kalinga, D. N., Bertoft, E., Tetlow, I., Liu, Q., Yada, R. Y., & Seetharaman, K. (2014). Evolution of amylopectin structure in developing wheat endosperm. *Carbohydrate Polymers*, *112*, 316–324.
Kalinga, D. N., Waduge, R., Liu, Q., Yada, R. Y., Bertoft, E., & Seetharaman, K. (2013). On the differences in the granular architecture and starch structure between pericarp and endosperm wheat starches. *Starch*, *65*, 791–800.
Klucinec, J. D., & Thompson, D. B. (1998). Fractionation of high-amylose maize starches by differential alcohol precipitation and chromatography of the fractions. *Cereal Chemistry*, *75*, 887–896.
Koch, K., Andersson, R., & Åman, P. (1998). Quantitative analysis of amylopectin unit chains by means of high-performance anion-exchange chromatography with pulsed amperometric detection. *Journal of Chromatography A*, *800*, 199–206.
Kong, X., Corke, H., & Bertoft, E. (2009). Fine structure characterization of amylopectins from grain amaranth starch. *Carbohydrate Research*, *344*, 1701–1708.
Kozlov, S. S., Blennow, A., Krivandin, A. V., & Yuryev, V. P. (2007). Structural and thermodynamic properties of starches extracted from GBSS and GWD suppressed potato lines. *International Journal of Biological Macromolecules*, *40*, 449–460.
Matheson, N. K. (1996). The chemical structure of amylose and amylopectin fractions of starch from tobacco leaves during development and diurnally–nocturnally. *Carbohydrate Research*, *282*, 247–262.
Matheson, N. K., & Wheatley, J. M. (1963). Diurnal–nocturnal changes in the starch of tobacco leaves. *Australian Journal of Biological Sciences*, *16*, 70–76.
Pérez, S., & Bertoft, E. (2010). The molecular structures of starch components and their contribution to the architecture of starch granules: A comprehensive review. *Starch*, *62*, 389–420.
Santacruz, S., Koch, K., Andersson, R., & Åman, P. (2004). Characterization of potato leaf starch. *Journal of Agricultural and Food Chemistry*, *52*, 1985–1989.
Santelia, D., & Zeeman, S. C. (2011). Progress in Arabidopsis starch research and potential biotechnological applications. *Current Opinion in Biotechnology*, *22*, 271–280.
Shiotsubo, T., & Takahashi, K. (1984). Differential thermal analysis of potato starch gelatinization. *Agricultural and Biological Chemistry*, *48*, 9–17.
Skeffington, A. W., Graf, A., Duxbury, Z., Gruissem, W., & Smith, A. M. (2014). Glucan, water dikinase exerts little control over starch degradation in *Arabidopsis* leaves at night. *Plant Physiology*, *165*, 866–879.
Smith, A. M. (2012). Starch in the Arabidopsis plant. *Starch*, *64*, 421–434.
Smith, A. M., & Zeeman, S. C. (2006). Quantification of starch in plant tissues. *Nature Protocols*, *1*, 1342–1345.
Stitt, M., & Zeeman, S. C. (2012). Starch turnover: Pathways regulation and role in growth. *Current Opinion in Plant Biology*, *15*, 282–292.
Szydlowski, N., Ragel, P., Hennen-Bierwagen, T. A., Planchot, V., Myers, A. M., Mérida, A., et al. (2011). Integrated functions among multiple starch synthases determine both amylopectin chain length and branch linkage location in *Arabidopsis* leaf starch. *Journal of Experimental Botany*, *62*, 4547–4559.
Vamadevan, V., Bertoft, E., & Seetharaman, K. (2013 a). On the importance of organization of glucan chains on thermal properties of starch. *Carbohydrate Polymers*, *92*, 1653–1659.
Vamadevan, V., Bertoft, E., Soldatov, D. V., & Seetharaman, K. (2013 b). Impact on molecular organization of amylopectin in starch granules upon annealing. *Carbohydrate Polymers*, *98*, 1045–1055.
Waduge, R. N., Kalinga, D. N., Bertoft, E., & Seetharaman, K. (2014). Molecular structure and organization of starch granules from developing wheat endosperm. *Cereal Chemistry* (in press).
Waduge, R. N., Xu, S., Bertoft, E., & Seetharaman, K. (2013). Exploring the surface morphology of developing wheat starch granules by using atomic force microscopy. *Starch*, *65*, 398–409.
Wang, T. L., Bogracheva, T. Y., & Hedley, C. L. (1998). Starch: As simple as A, B, C? *Journal of Experimental Botany*, *49*, 481–502.
Wattebled, F., Planchot, V., Dong, Y., Szydlowski, N., Pontoire, B., Devin, A., et al. (2008). Further evidence for the mandatory nature of polysaccharide debranching for the aggregation of semicrystalline starch and for overlapping functions of debranching enzymes in Arabidopsis leaves. *Plant Physiology*, *148*, 1309–1323.
Wikman, J., Larsen, F. H., Mohammed, S. M., Blennow, A., & Bertoft, E. (2011). Phosphate esters in amylopectin clusters of potato tuber starch. *International Journal of Biological Macromolecules*, *48*, 639–649.
Zeeman, S. C., Kossmann, J., & Smith, A. M. (2010). Starch: Its metabolism, evolution and biotechnological modification in plants. *Annual Review of Plant Biology*, *61*, 209–234.
Zeeman, S. C., Smith, S. M., & Smith, A. M. (2007). The diurnal metabolism of leaf starch. *Biochemical Journal*, *401*, 13–28.

Zeeman, S. C., Tiessen, A., Pilling, E., Kato, K. L., Donald, A. M., & Smith, A. M. (2002). Starch synthesis in Arabidopsis. Granule synthesis, composition and structure. *Plant Physiology*, *129*, 516–529.

Zhu, F., Bertoft, E., & Seetharaman, K. (2013). Characterization of internal structure of maize starches without amylose and amylopectin separation. *Carbohydrate Polymers*, *97*, 475–481.

Zhu, F., Bertoft, E., Källman, A., Myers, A. M., & Seetharaman, K. (2013). Molecular structure of starches from maize mutants deficient in starch synthase III. *Journal of Agricultural and Food Chemistry*, *61*, 9899–9907.

Zhu, F., Bertoft, E., & Seetharaman, K. (2014). Distribution of branches in whole starches from maize mutants deficient in starch synthase III. *Journal of Agricultural and Food Chemistry*, *62*, 4577–4583.